Mesomorphic Transition of a Thermotropic Polyester with Biphenylyl Mesogen under Hydrostatic Pressure

Yoji Maeda*,† and Junji Watanabe‡

National Institute of Materials and Chemical Research, 1-1 Higashi, Tsukuba, Ibaraki 305, Japan, and Department of Polymer Chemistry, Tokyo Institute of Technology, Ookayama, Meguro-ku, Tokyo 152, Japan

Received July 1, 1994; Revised Manuscript Received November 10, 1994®

ABSTRACT: The phase transition of a thermotropic (4,4′-dihydroxybiphenylyl)tetradecanedioic acid polyester (PB-12) was studied using wide-angle X-ray scattering and differential thermal analysis (DTA) under hydrostatic pressures up to 300 MPa. The corrected T vs P phase diagram of the PB-12 polyester was constructed by a high-pressure DTA method. The typical phase transition of crystal (K)–smectic H (S_H)–isotropic melt (I) was observed under hydrostatic pressures up to 90–100 MPa. At high pressures above about 100–120 MPa, however, a new smectic phase, clearly different from the usual S_H phase, is found at high temperatures and a different transition process of K–new smectic phase–I can be observed at elevated pressures. The new smectic phase is also formed irreversibly from the usual S_H phase by increasing pressure on a quasi-isothermal process. The pressure-induced smectic phase was assigned to be a smectic B (S_B) phase because the d spacing of the low-angle reflection corresponds to the extended length of the PB-12 molecule, suggesting the arrangement of the molecules vertical to the smectic layer, and also a single reflection at the wide-angle region, suggesting a hexagonal packing. The S_B phase was partly supercooled at high pressures, and the glassy S_B phase coexistent with the normal crystals was analyzed under atmospheric pressure.

Introduction

The studies of the effect of pressure on low molecular mass liquid crystals have been extensively performed since the 1970s.[1–5] Cladis and Goodby[3,4] studied the effect of pressure on the phase transition of interesting low molecular weight liquid crystals such as *N*-[4-(*n*-butyloxy)benzylidene]-4-*n*-octylaniline (4O.8) and *n*-hexyl 4′-(*n*-pentyloxy)biphenyl-4-carboxylate (65OBC), which show a smectic B phase in both samples. The pressure-induced liquid crystallinity of low molecular weight samples was reviewed by Chandrasekhar et al.[6,7] An important conclusion from the reviews was that the isotropic liquids of anisotropic molecules can be transformed into mesophases at elevated pressures. For the study of a pressure-induced mesomorphic transition in polymers, main-chain thermotropic polyesters are interesting since significant pressure effects might be expected because of the alternate arrangement of the rigid mesogenic core and the flexible aliphatic spacer in the repeating unit. There are several studies of pressure-induced liquid crystallinity for polymers. For example, Samulski et al.[8,9] reported two interesting pressure effects, a pressure-induced crystal habit and a pressure-induced mesophase, of the aromatic copolyester, HIQ-20, composed of 20% hydroxybenzoic acid, 40% isophthalic acid, and 40% hydroquinone. Maeda et al.[10,11] reported the effect of pressure on the structure and thermal property of poly(4,4′-dioxy-2,2′-dimethylazoxybenzene–dodecanedioyl) (labeled as DDA-9) in which crystalline polymorphs are found under pressures above about 50 MPa. Furthermore, Maeda and Watanabe[12] reported that a pressure-induced mesomorphism of (4,4′-dihydroxybiphenylyl)tetradecanedioic acid polyester, PB-12, is found using wide-angle X-ray scattering (WAXS) under hydrostatic pressures. The main-chain thermotropic polyester of PB-12, based on the 4,4′-dihydroxybiphenylyl unit as a mesogen and the aliphatic dibasic acid with 12 methylene units as a flexible spacer, shows a mesophase of the smectic H (S_H) type in a relatively broad temperature region between the crystalline solid and the isotropic melt at atmospheric pressure.[13–15] According to Gray and Goodby's definition of smectic liquid crystals, the S_H phase is a smectic phase in which the molecules have their longer axes tilted with respect to the normal to the layer plane.[16] The chemical structure is shown:

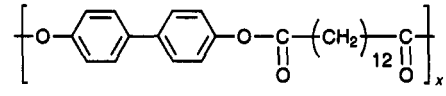

The same structural behavior of the crystal (K)–S_H phase transition as the one at atmospheric pressure was observed under hydrostatic pressures up to 90 MPa.[12] Further increase of the pressure above about 100 MPa, on the other hand, results in a quite different change in the WAXS profiles at the K–S_H transition. The S_H phase observed in the low-pressure region below 90 MPa altered to form a new smectic phase at high pressures above 100–120 MPa. The new smectic phase was suggested to be either a smectic B (S_B) or a smectic E (S_E) phase. Molecules in the S_B and S_E phases are arranged within the layers in a hexagonally close-packed or orthorhombic array with the molecular long axes perpendicular to the layer plane, respectively.[16] The phase diagram constructed by the high-pressure X-ray study indicates the stable regions between the crystal, S_H phase, S_B (or S_E) phase, and isotropic molten phase.[12]

In this study, the structural and thermal behavior of the phase transition was investigated further, especially the pressure-induced mesomorphism, of the PB-12 polyester by using the WAXS apparatus, equipped with both a high-pressure sample vessel and a PSPC–MCA data acquisition system, and a high-pressure differential thermal analysis (DTA) apparatus.[17,18] The characterization of the resultant pressure-crystallized samples

* Author to whom correspondence is addressed.
† National Institute of Materials and Chemical Research.
‡ Tokyo Institute of Technology.
® Abstract published in *Advance ACS Abstracts,* January 15, 1995.

0024-9297/95/2228-1661$09.00/0

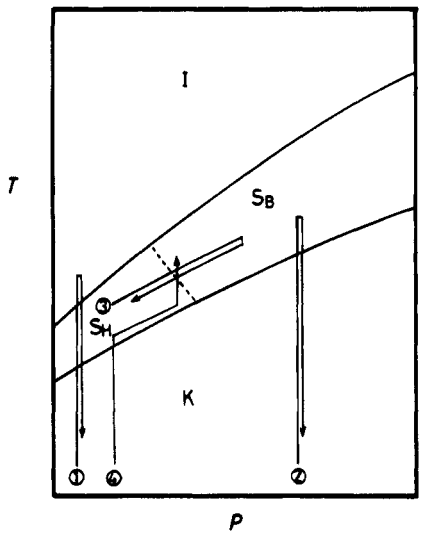

Figure 1. WAXS measuring processes of the PB-12 polyester. Routes 1 and 2 show isobaric processes, for example, at 20 and 300 MPa. Route 3 shows a quasi-isothermal process of crossing over the boundary between the S_H and S_B phases from 50 to 150 MPa. Route 4 shows a heating process at 95 MPa of the S_H phase formed at 50 MPa.

was performed by using differential scanning calorimetry (DSC) and wide-angle X-ray scattering at atmospheric pressure.

Experimental Section

Characterization. The PB-12 polyester used in this study is described elsewhere.[13-15] The inherent viscosity of the sample was 0.75 dL/g, which was determined at 25 °C using a 0.5 g/dL solution in a 60/40 mixture by weight of phenol and tetrachloroethane. The transition points of the PB-12 sample at atmospheric pressure are K 198 °C → S_H 231 °C → I, where K denotes the crystal, S_H the smectic H phase, and I the isotropic molten phase, respectively.

The X-ray structural change of the PB-12 polyester on isobaric and quasi-isothermal processes was measured at hydrostatic pressures up to 300 MPa by using the WAXS apparatus equipped with the high-pressure sample vessel that was previously developed in our laboratory.[11,17] The dimethylsilicone oil with low viscosity (10 cSt) was used as the pressure medium.

Thermal behavior of the PB-12 polyester under hydrostatic pressures was measured at pressures up to 400 MPa by using the high-pressure DTA apparatus which was already reported elsewhere.[17,18] The DTA measurements were performed at a constant rate of 5 °C/min at all pressures. Temperature measured with C–A thermocouples was calibrated to be within the error of ±0.5 °C. Samples were coated with epoxy adhesive in order to fix the sample tight at the bottom of platinum sample holder and also to inhibit direct contact with the silicone oil as the pressure medium.

The thermal behavior of the resultant pressure-crystallized samples was measured by using a Perkin-Elmer DSC-II apparatus. The scanning rate was constant at 10 °C/min. Temperature and heat of fusion were calibrated with a standard material of indium.

Results and Discussion

Pressure-Induced Smectic Phase. X-ray structural measurements of the phase transition of the PB-12 polyester were performed on the four different processes that are schematically illustrated on the T vs P phase diagram in Figure 1.[12] Routes 1 and 2 are isobaric processes for the measurement of the phase transitions of K–S_H–I and K–S_B on heating and subsequent cooling at 20 and 200 MPa, respectively. Route 3 is a quasi-isothermal process for the measurement of the mesomorphic transition between the S_H and the pressure-induced smectic S_B phases at temperatures just above the K–S transition curve. This was performed to study whether the mesomorphic transition occurs reversibly or not in the pressure region between 50 and 150 MPa. Route 4 is another process for observing the mesomorphic transition from the S_H to S_B phases on heating at a constant pressure. The main object of routes 3 and 4 is to observe directly how the starting S_H phase is transformed into the S_B phase through the boundary region of 90–120 MPa.

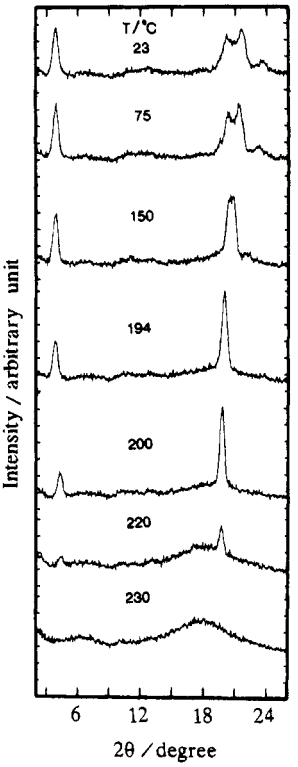

Figure 2. WAXS patterns of the PB-12 polyester on heating at 20 MPa.

Figure 2 shows the WAXS patterns of the PB-12 sample on heating at 20 MPa. The X-ray profiles show the same K–S_H–I phase transition as the one observed at atmospheric pressure, and the structural changes are observed to be reversible. The typical WAXS pattern of the crystal at room temperature shows a sharp low-angle reglection at $2\theta = 3.9_8°$, two strong wide-angle reflections at ca. $20.2_4°$ and $21.7_2°$, and a weak reflection at $23.4_0°$. In the crystalline state the low-angle reflection changes slightly with temperature, while the two strong wide-angle reflections change significantly with increasing temperature. The two wide-angle reflections are merged to a single reflection of $2\theta = 20.4_6°$ (4.3$_4$ Å) at about 165 °C. The strong low-angle and the merged wide-angle reflections are observed in the high-temperature region above 165 °C. As the K–S_H transition occurs at 200 °C, the low-angle reflection shifts discontinuously to a wider angle and the merged wide-angle reflection shifts gradually. The d spacing of the low- and wide-angle reflections of the PB-12 sample at 20 MPa is plotted as a function of temperature in Figure 3. The d spacing of the low-angle reflection shifts abruptly from 23.3$_9$ Å ($2\theta = 3.7_8°$) to 20.9$_0$ Å ($2\theta = 4.2_3°$) at the K–S_H transition, while the d spacing of the wide-angle reflection at 200 °C is about 4.5$_0$ Å ($2\theta = 19.7_4°$) and it changes continuously at the K–S_H transition. In the S_H phase, the d spacing of the former reflection is

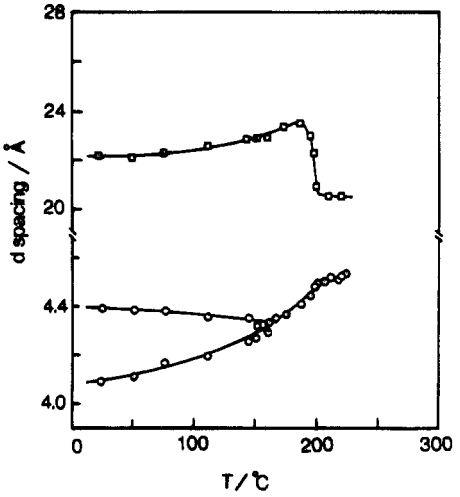

Figure 3. Temperature dependence of the d spacing of the low- and wide-angle reflections at 20 MPa.

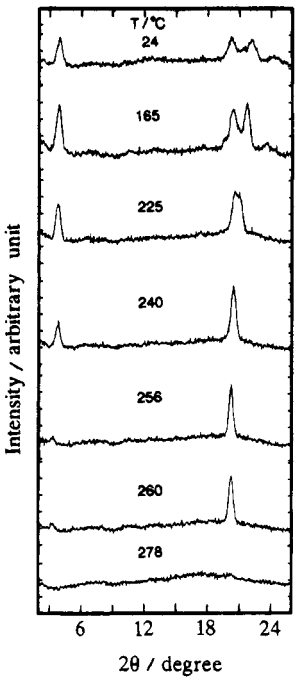

Figure 4. WAXS patterns of the PB-12 polyester on heating at 300 MPa.

almost constant, while that of the latter increases linearly with temperature. The same structural behavior was observed under hydrostatic pressures up to 90 MPa.

An entirely different behavior of the low-angle reflection is observed at the K–S transition under hydrostatic pressures above 100–120 MPa: i.e., the trend is obviously opposite to that observed at low pressures, indicating that a new smectic phase is formed.[12] Figure 4 shows the structural change of the WAXS patterns on heating at 300 MPa. The structural behavior in the crystalline state is very similar to those at low pressures. The major difference in the WAXS patterns at 20 and 300 MPa is the behavior of the low-angle reflection during the K–S transition. The low-angle reflection at 300 MPa shifts discontinuously from $2\theta = 3.8_7°$ to a weak reflection at a smaller angle of $2\theta = 3.3_7°$. It is also noted that the low-angle reflection of the S_B phase is relatively weak in comparison to that of the S_H phase. Figure 5 shows the change in the d spacing of the low- and wide-angle reflections of the PB-12 polyester at 300 MPa. The d spacing of the low-angle reflection increases by about 3.3 Å from 22.8_5 to 26.2_0 Å at the K–S transition, in contrast to the decrease in the d spacing of about 2.5 Å at 20 MPa. The structural behavior of the wide-angle reflections is apparently similar to those in the low-pressure region, except that the merging of the two wide-angle reflections at $2\theta \approx 20–21°$ is shifted to a relatively high temperature (235 °C) just below the K–S transition point (244 °C). This suggests that hydrostatic pressure has a remarkable effect of suppressing the intermolecular motions in the side packing of the PB-12 crystals at high pressures. The new smectic phase is reduced to the smectic B (S_B) phase because the existence of a single reflection in the wide-angle region suggests a hexagonal packing[19] and the observed d spacing (26.2–26.9 Å) of the low-angle reflection corresponds well to the molecular length (ca. 27 Å) of the repeating unit in the extended chain conformation. Accordingly, it is reasonable to consider that the molecules in the pressure-induced smectic S_B phase lie almost perpendicular to the smectic layer, while the molecules in the S_H phase are tilted to the smectic layer. The S_B mesophase of the PB-12 polyester can be detected in the high pressures between 100–120 and 300 MPa, the highest pressure at which the X-ray measurement was performed. The observed data of the d spacing for the crystals and the two smectic phases of the PB-12 polyester are already reported.[12]

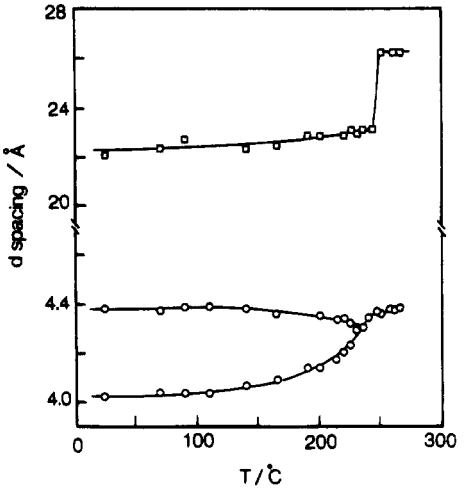

Figure 5. Temperature dependence of the d spacing of the low- and wide-angle reflections at 300 MPa.

Phase Diagram. Figure 6 shows the T vs P phase diagram of the PB-12 polyester that was constructed by the isobaric WAXS measurements such as routes 1 and 2 in Figure 1. The K–S transition curve is divided reasonably into two linear lines of the K–S_H and the K–S_B transition in the low- and high-pressure regions, respectively. The former line is located in the low-pressure region below about 120 MPa, and the other is in the higher pressure region. The boundary pressure between the K–S_H and the K–S_B transitions is ca. 100–120 MPa. Also one can see clearly an inflection of the S–I transition curve at about 100 MPa; i.e., the S–I line in the low-pressure region is for the S_H–I transition, and the other S–I line in the high-pressure region is for the S_B–I transition. These experimental facts are due to the difference in dT/dP of the corresponding transitions between the ordinary S_H phase and the pressure-induced S_B phases mentioned in the last section. The inflection point in both the K–S and S–I transition curves was indistinct in the phase diagram

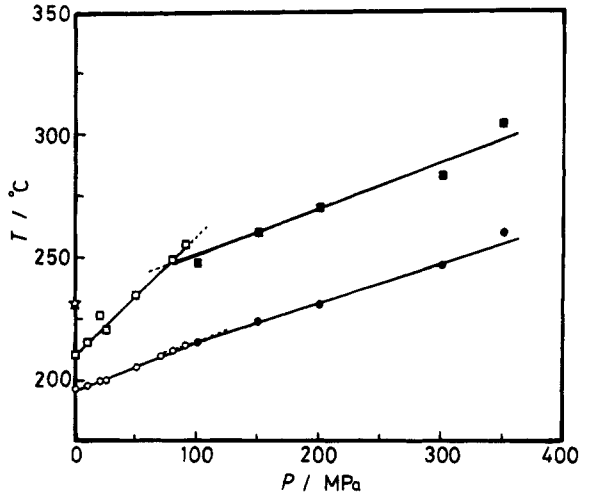

Figure 6. Phase diagram of the PB-12 polyester made by the high-pressure WAXS system. Open symbols of circles and rectangles indicate the K–S_H and S_H–I transitions, and filled symbols of the circles and rectangles indicate the K–S_B ad S_B–I transitions, respectively.

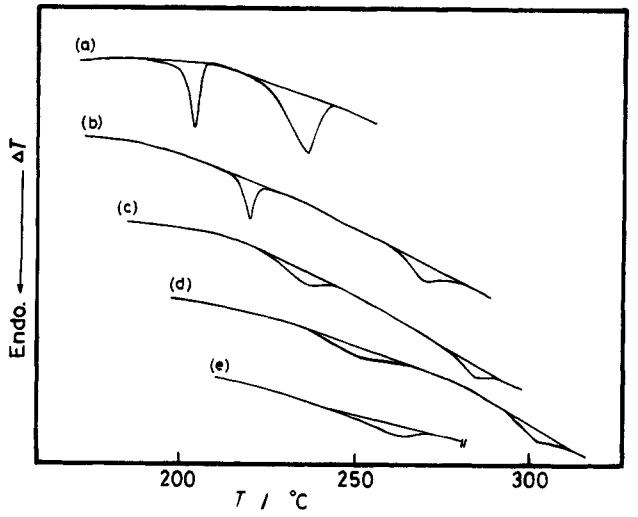

Figure 7. High-pressure DTA curves of the original PB-12 sample: (a) 20, (b) 100, (c) 200, (d) 300, and (e) 400 MPa.

reported before,[12] because of the small amount of data in the low-pressure region.

Another important point is the construction of the T vs P phase diagram. The K–S_H and S_H–I transition points at atmospheric pressure can be extrapolated approximately to 198 and 210 °C, respectively, in Figure 6. However, the DSC curve indicates that the K–S_H and S_H–I transition temperatures are observed at 198.2 and 234.8 °C, respectively. There is a large discrepancy in the S_H–I transition point which is much greater than the experimental errors of ±0.5 °C. In order to construct the accurate phase diagram, the high-pressure DTA measurements were performed in which the PB-12 sample was coated by epoxy adhesive because the contact with the silicone oil as the pressure medium can be avoided. Figure 7 shows the DTA heating curves of the PB-12 sample under pressures up to 400 MPa. The DTA curve at 20 MPa shows the same K–S_H and S_H–I transitions as those in the DSC curves. The endothermic peak of the K–S_H transition is sharp at pressures up to 100 MPa, while the peak has broadened at high pressures above about 150–200 MPa. The peak temperatures of the K–S and S–I transitions are plotted as a function of pressure in Figure 8. The phase

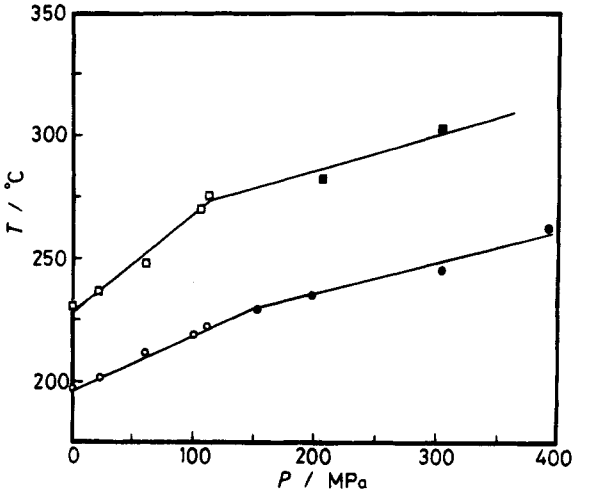

Figure 8. Phase diagram of the PB-12 sample made by high-pressure DTA. Symbols are the same as those in Figure 6.

diagram of the PB-12 sample shows qualitatively the same pattern in Figure 6; there is an inflection at 120–150 MPa in both the K–S and S–I transition curves. The evidence of inflection in the K–S and S–I transition curves supports the WAXS experimental fact on the existence of the S_B phase under hydrostatic pressures above 100–120 MPa. Compared with the phase diagram in Figure 6, the K–S_H and K–S_B transition lines in Figure 8 are in good agreement with those in Figure 6. However, the S–I transition points in Figure 8 are ca. 20° higher than the corresponding S–I points in Figure 6. Accordingly, the discrepancy can be explained by the depression of the S–I transition point due to a miscible interaction between the smectic phase and the silicone oil as the pressure medium. The K–S and S–I transition curves in Figure 8 should be appropriate for the accurate T vs P phase diagram of the PB-12 polyester. The pressure dependence of the K–S and S–I transitions in the low- and high-pressure regions can be well expressed as a first-order polynomial of pressure in the following.

$$\text{MPa} \le P \le 90 \text{ MPa}$$

$$\text{K–}S_H \text{ transition: } T = 197.6 + 0.21_2P$$

$$S_H\text{–I transition: } T = 229.5 + 0.42_4P$$

$$P \ge 100\text{–}120 \text{ MPa}$$

$$\text{K–}S_B \text{ transition: } T = 206.8 + 0.14_4P$$

$$S_B\text{–I transition: } T = 251.5 + 0.16_9P$$

The K–S_H and S_H–I transition lines in the low-pressure region are found to be consistent with those of the same series of polyesters of PB-10, PB-14, and PB-18 which will be published in the near future. It should be emphasized here that the appearance of the smectic S_B phase of the PB-12 polyester at pressures above about 120 MPa is independent of whether the sample is in contact with the silicone oil or not. Cladis and Goodby[4] reported the P vs T phase diagram of the 65OBC sample in which the S_A–S_B (hexatic B) transition line becomes steeper above 1.5 kbar. They explained that, at higher pressures, positional correlations become stronger as the intermolecular distance is decreased and so the hexatic B transforms to the crystal B at higher pressures. Although the pressure-induced S_H–S_B transition of the

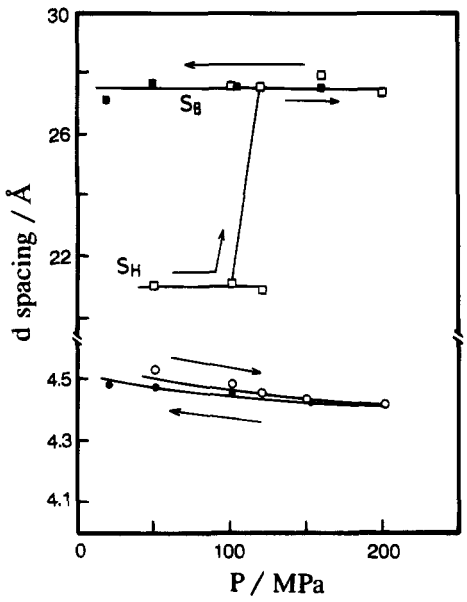

Figure 9. Change in the d spacing of the low- and wide-angle reflections during the irreversible transition between the S_H and S_B phases of the PB-12 sample along route 3. Open and filled symbols are data on pressurizing and depressurizing processes, respectively.

PB-12 polyester in this study is different from the transition of the 65OBC sample, the S_B phase of the PB-12 sample might be classified to the crystal B phase.

Mesomorphic Transition between Smectic H and Smectic B Phases. It is estimated from Figures 6 and 8 that the phase boundary between the S_H and S_B phases is located at pressures between 90 and 120 MPa. The smectic phases can be distinguished clearly from each other through the 2θ angle (or d spacing) of the low-angle reflection: $2\theta \approx 4.2°$ (20.9 Å) for the S_H phase and $2\theta \approx 3.3°$ (26.5 Å) for the S_B phase.

The mesomorphic transition between the S_H and S_B phases of the PB-12 sample was studied by increasing the pressure and subsequent pressure-releasing along the route 3 process. Route 3 starts from the S_H phase at 210 °C and 50 MPa to the S_B phase at 235 °C and 200 MPa on a quasi-isothermal (T_{K-S} + 5 °C) process. Figure 9 shows the change in the d spacing of the low- and wide-angle reflections of the S_H phase on pressurizing and the subsequent depressurizing processes. The S_H phase is transformed discontinuously to the S_B phase from 218 °C and 90 MPa to 221 °C and 120 MPa on the pressurizing process. Once the S_B phase is formed, it is not reversible during releasing the pressure. The S_B phase was maintained even after annealing the sample at 198 °C and 1 MPa for 2 h. The S_B phase was transformed either to the crystals by cooling or to the isotropic melt by heating at 1 MPa. It is noted that the S_B phase at low pressures such as 1 MPa may be metastable at the mesophase temperatures. Another experiment of the phase transformation of the S_H phase was performed on heating at 95 MPa along the route 4 process. The procedure was as follows: first, the sample was heated to the smectic S_H phase at 50 MPa. Then, the S_H phase at 205 °C and 50 MPa was pressurized at 216 °C and 95 MPa along the K–S_H transition curve, and finally the S_H phase was heated slowly from 216 °C to the isotropic molten state at 95 MPa. The typical WAXS pattern of the S_H phase at 216 °C and 95 MPa shows low- and wide-angle reflections at $2\theta = 4.0_9°$ (21.5$_9$ Å) and 19.7$_4$° (4.5$_0$ Å), respectively. On gradual heating above 220 °C, a new low-angle reflection appears at $2\theta = 3.2_1°$ (27.4$_8$ Å), while the usual low-angle reflection of the S_H phase becomes weak with temperature and it disappears at about 227 °C. The same structural change as those in Figure 9 is observed on heating in the isobaric process, and the process is an irreversible transition. Figure 10 shows the schematic molecular arrangements between the crystal and the smectic S_H and S_B phases depending upon the condition of temperature and pressure.

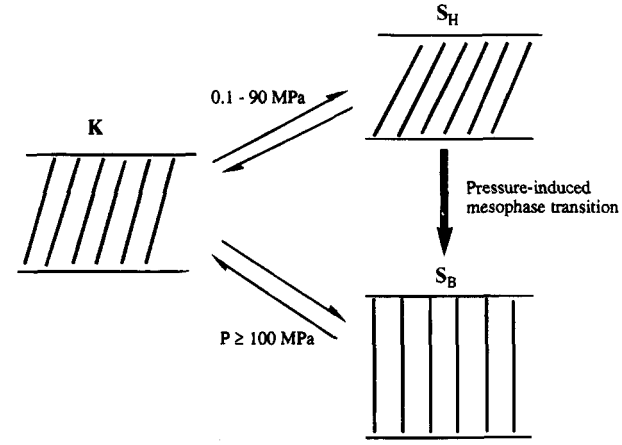

Figure 10. Schematic arrangements of molecules in the crystal, the S_H, and the S_B phases of the PB-12 polyester.

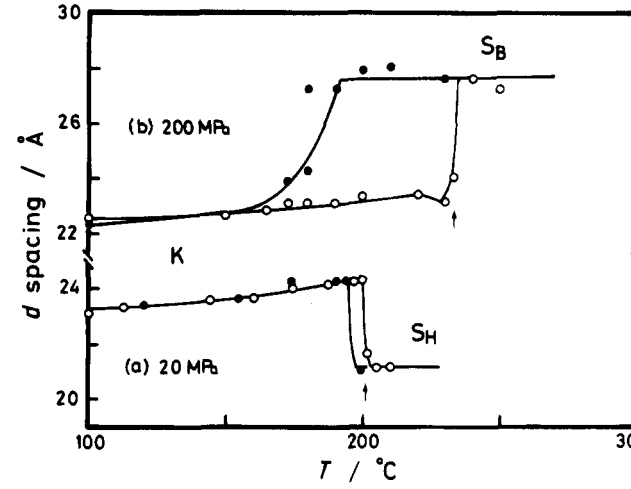

Figure 11. Change in the d spacing of the low-angle reflection on cooling from the S_H and S_B phases at 20 and 200 MPa, respectively. Open and filled circles are data on heating and cooling processes at each pressure.

Crystallization behavior of the PB-12 sample at 20 and 200 MPa was monitored to compare the habits of crystallization from the two smectic mesophases. Figure 11 shows the change in the d spacing of the low-angle reflection on cooling and subsequent heating processes at 20 and 200 MPa, respectively. The S_H phase at 20 MPa is crystallized rapidly with small degrees of supercooling of approximately $\Delta T \sim 5–7$ °C. However, at 200 MPa, the S_B phase has a very large degree of supercooling of $\Delta T \sim 30–40$ °C and was crystallized only at small rates of cooling (0.2–0.4 °C/min). This strongly suggests that the S_B phase under high pressures is easily supercooled to a glassy S_B phase by cooling at normal rates, for example, at 5 °C/min.

Characterization of the Quenched Samples. Figure 12 shows the WAXS pattern and the Laue photograph at atmospheric pressure of the S_B phase-rich sample cooled rapidly (~10 °C/min) at 150 MPa. The WAXS pattern shows clearly two low-angle reflections

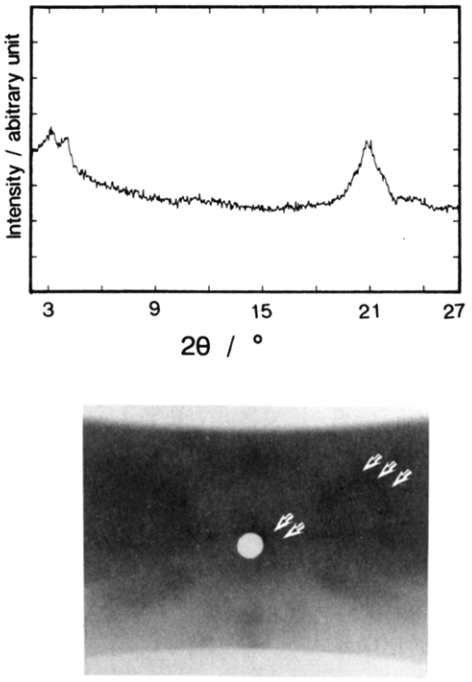

Figure 12. WAXS pattern and Laue photograph at 23 °C and atmospheric pressure of the PB-12 sample cooled rapidly at 150 MPa.

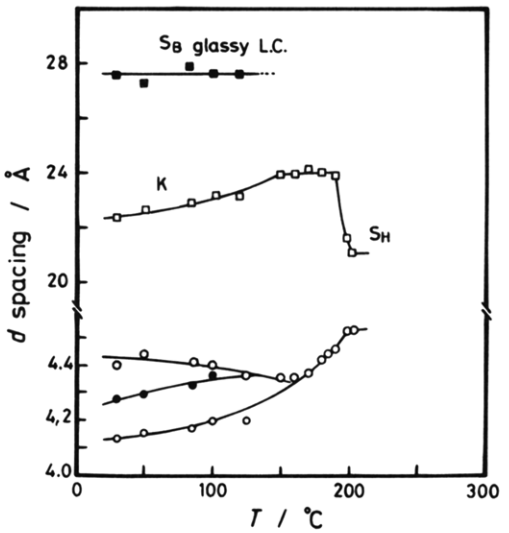

Figure 13. Change in the d spacing of the reflections on heating at atmospheric pressure of the PB-12 sample cooled rapidly at 150 MPa. Open and filled symbols are for the crystal and the glassy S_B phase, respectively.

at $2\theta = 3.2_4°$ (27.2$_9$ Å) and $3.8_7°$ (22.8$_5$ Å) belonging to the S_B phase and the crystals, respectively, and an overlapped broad peak at about 21°. The Laue photograph also shows two Debye rings at low angles in addition to three reflections at wide angles. The broad peak at wide angles consists of three reflections: the main peak at $2\theta = 20.8_0°$ (4.2$_6$ Å) of the supercooled S_B phase and the two shoulder peaks at $2\theta = 20.1_9°$ (4.4$_0$ Å) and $21.8_1°$ (4.0$_7$ Å) of the crystals. The experimental facts indicate clearly the coexistence of the crystal and supercooled S_B phase at room temperature under atmospheric pressure. It is interesting to carry out studies on the thermal stability of the supercooled S_B phase at atmospheric pressure. Figure 13 shows the change in the d spacing of the WAXS pattern under atmospheric pressure of the sample cooled rapidly at 150 MPa. On the gradual heating, the low-angle

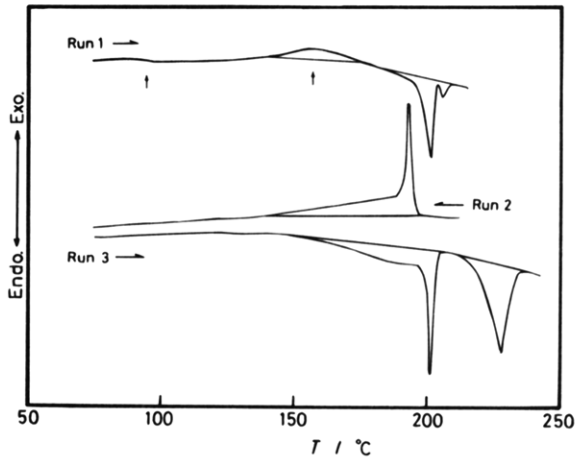

Figure 14. DSC heating curves of the PB-12 sample cooled rapidly at 150 MPa (run 1), subsequent cooling (run 2), and reheating (run 3) curves. Scanning rate: 10 °C/min.

Table 1. Thermodynamic Data of Phase Transitions of the PB-12 Polyester

	exothermic peak		K–S_H transition		S_H–I transition	
sample	T/K	ΔH/(J g^{-1})	T/K	ΔH/(J g^{-1})	T/K	ΔH/(J g^{-1})
normal samples						
formed at 0.1 MPa			472	13.0–14.6	507	33.9
formed at 20 MPa			473	9.8	493	34.5
run 1 (quenched at 150 MPa)						
	433	4.2	473	8.8 + 1.6		
	435	5.8	472	7.6 + 1.0	496	20.4
run 3 (2nd heating)			474	10.7	501	35.6

reflection of the supercooled S_B phase is held unchanged at temperatures up to 120 °C. The whole reflections of the supercooled S_B phase become ambiguous with increasing temperature, and finally they disappear at about 140–150 °C. On the other hand, the d spacing of the usual low-angle reflection of the coexistent crystals increases gradually by about 1–2 Å from room temperature to about 150 °C. On further heating above 150 °C, the WAXS reflections become sharp and its pattern is typical of crystals at high temperatures. The resultant crystals are transformed to the isotropic melt via the typical S_H phase at about 200 °C. The DSC measurements of the same sample were performed to confirm the glass transition and cold crystallization of the supercooled S_B phase. Figure 14 shows the DSC curves at 10 °C/min of the quenched sample. Run 1 shows the DSC curve of the quenched sample on heating up to temperatures just above the K–S_H point, then run 2 shows the cooling curve from the S_H phase, and run 3 indicates the reheating curve of the sample cooled by run 2. In run 1, the glass-transition-like behavior is observed slightly at about 95 °C, and a broad but small exothermic peak is observed clearly around 160 °C. The appearance of an exothermic peak around 160 °C corresponds well to the structural change of the disappearance of the low- and wide-angle reflections of the supercooled S_B phase. Accordingly, the supercooled S_B phase can be ascribed to the smectic S_B glass and the exothermic peak is due to the cold crystallization of the smectic S_B glass on heating. The enthalpy of the exothermic peak is estimated to be about 4.2–5.8 J/g. The K–S_H transition showed a large endothermic peak at 200.6 °C and an additional peak at 206 °C, suggesting the melting (K–S transition) of the crystals formed by

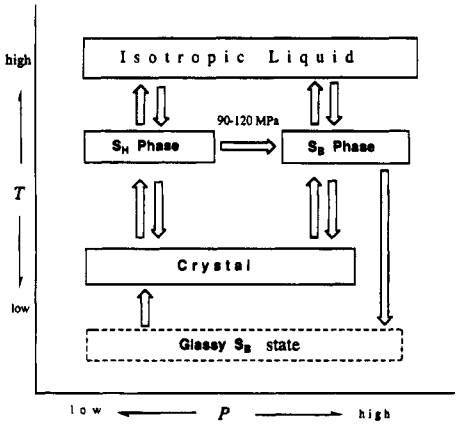

Figure 15. Schematic diagram of the phase transitions of the PB-12 polyester.

cold crystallization and the original crystals formed at 150 MPa, respectively. The total enthalpy of the K–S_H transition was estimated to about 10.0 J/g, including the enthalpy of the additional subpeak of 1.0–1.6 J/g. Run 3 shows the typical K–S_H–I transition behavior of the PB-12 polyester. The thermodynamic data on the phase transition of the PB-12 polyester are listed in Table 1. From these results, it is reasonable to consider that the glassy S_B sample is formed by cooling rapidly at high pressures and that it is transformed into the crystals via cold crystallization at about 130–160 °C on heating. In summary, the phase relationship between the crystal, the S_H phase, the S_B phase, and the isotropic melt of the PB-12 polyester is schematically shown in Figure 15.

Conclusion

The phase behavior of the PB-12 polyester is summarized in the following. First, the typical K–S_H–I phase transition occurs reversibly in the low-pressure region below 90–100 MPa. Second, the pressure-induced smectic phase is formed in place of the usual S_H phase at high pressures above 100–120 MPa. It is identified as the smectic B (S_B) phase because the new smectic phase shows only a reflection in the wide-angle region, indicating the hexagonal packing, and the *d* spacing of the low-angle reflection corresponds to the extended-chain length of the PB-12 molecule, suggesting the molecular arrangement normal to the smectic layer. The K–S_B–I phase transition occurs reversibly at high pressures above 120 MPa. Third, the S_H phase is transformed irreversibly to the S_B phase at pressures between 90 and 120 MPa by applying pressure at mesophase temperatures. Fourth, the S_B phase is easily supercooled at high pressures and then is quenched to a glassy S_B phase. The usual S_H phase is crystallized too fast to obtain the glassy S_H state at low pressures including atmospheric pressure. The glassy S_B sample was analyzed at atmospheric pressure by WAXS and DSC methods. The quenched sample shows a glass transition at ca. 95 °C and an exothermic peak at about 140–170 °C on the DSC curve, which is identified as the cold crystallization of the glassy S_B phase.

References and Notes

(1) Keyes, P. H.; Weston, H. T.; Daniels, W. B. *Phys. Rev. Lett.* **1973**, *31*, 628.
(2) Lin, W. J.; Keyes, P. H.; Daniels, W. B. *Phys. Lett.* **1974**, *49A*, 453.
(3) Cladis, P. E.; Goodby, J. W. *Mol. Cryst. Liq. Cryst.* **1982**, *72*, 307.
(4) Cladis, P. E.; Goodby, J. W. *Mol. Cryst. Liq. Cryst.* **1982**, *72*, 313.
(5) Rübesamen, J.; Schneider, G. M. *Liq. Cryst.* **1993**, *13*, 711.
(6) Chandrasekhar, S.; Ramaseshar, S.; Reshamwala, A. S.; Sadashiva, B. K.; Shashidhar, R.; Surendranath, V. *Liq. Cryst., Proc. Int. Conf.* **1975**, *1*, 117.
(7) Chandrasekhar, S.; Shashidhar, R. *Advances in Liquid Crystals*; Brown, G. H., Ed.; Academic Press: New York, 1979; Vol. 4, Chapter 2.
(8) Hsiao, B. S.; Shaw, M. T.; Samulski, E. T. *Macromolecules* **1988**, *21*, 543.
(9) Hsiao, B. S.; Shaw, M. T.; Samulski, E. T. *J. Polym. Sci., Polym. Phys. Ed.* **1990**, *28*, 189.
(10) Maeda, Y.; Blumstein, A. *Mol. Cryst. Liq. Cryst.* **1991**, *195*, 169.
(11) Maeda, Y.; Tanigaki, N.; Blumstein, A. *Mol. Cryst. Liq. Cryst.* **1993**, *237*, 407.
(12) Maeda, Y.; Watanabe, J. *Macromolecules* **1993**, *26*, 401.
(13) Asrar, J.; Toriumi, H.; Watanabe, J.; Krigbaum, W. R.; Ciferri, A. *J. Polym. Sci., Polym. Phys. Ed.* **1983**, *21*, 1119.
(14) Krigbaum, W. R.; Watanabe, J.; Ishikawa, T. *Macromolecules* **1983**, *16*, 1271.
(15) Watanabe, J.; Krigbaum, W. R. *Macromolecules* **1984**, *17*, 2288.
(16) Gray, G. W.; Goodby, J. W. G. *Smectic Liquid Crystals*; Leonard Hill: Glasgow, Scotland, 1984; Chapters 2, 5, and 8.
(17) Maeda, Y.; Kanetsuna, H. *Bull. Res. Inst. Polym. Text. (Jpn.)* **1985**, *149*, 119.
(18) Maeda, Y. *Thermochim. Acta* **1990**, *163*, 211.
(19) Luckhurst, G. R.; Gray, G. W. *The Molecular Physics of Liquid Crystals*; Academic Press: New York, 1979; pp 263–284.

MA941200W